

OPTIMIZED CLT-RC FRAME CONNECTION FOR SEISMIC RETROFITTING

Zabih Mehdipour¹, Jorge M. Branco², Elisa Poletti³, Paulo B. Lourenço⁴

ABSTRACT: Cross-laminated timber (CLT) panels have been used as a renovation solution to be adopted in existing masonry-infilled RC buildings, especially those which were designed based on old seismic codes. The connections through which the panels are attached to the RC frames have shown to provide the most contribution to the seismic behaviour of buildings, highly depending on the type of connections used. In this study, to investigate the effect of design procedures of bilinear RC-CLT connections on the dissipated energy and peak displacement of the retrofitted building, their optimum number, location, and mechanical properties, including elastic/inelastic stiffness and yielding displacement, are aimed to be found using genetic algorithm in a one-bay one-story RC frame. Two structures, (1) a masonry-infilled frame strengthened by CLT panel and (2) a CLT-infilled frame, are used to take the effect of masonry infill into account for two optimization purposes, maximum energy dissipation and minimum structural drift. Results show that under different predefined levels of structural performance, different optimum bilinear curves are achieved. In a parallel study, concerning connectors' arrangement, it was found that their horizontal distribution in beams, starting from the middle and moving to the corners, result in a much better response than a vertical distribution in columns.

KEYWORDS: Cross-laminated timber panel, Infilled RC frame, CLT-RC connection, Optimization, Genetic algorithm

1 INTRODUCTION

Cross-laminated timber (CLT) shear walls have developed recently as an infill added to existing buildings [1][2]. These buildings, mainly made of reinforced concrete frames infilled with masonry walls, have shown to be vulnerable to seismic actions due to in-plane and out-of-plane failures of the infills and shear failure of RC columns [3][4]. CLT panels added to those frames are able to improve elastic response with increasing stiffness and load-carrying capacity and inelastic response with ductile deformations and limited impairment of strength at the same time. Elastic contribution of the walls are made by the panels which are rigid due to their layers arranged crosswise to each other at an angle of 90° [5][6]. On the other hand, inelastic behaviour is improved only by the connections where CLT is attached to the frame [5][7][8]. Many traditional and innovative RC-CLT connections have been suggested to demonstrate their abilities to improve the main frame responses emphasizing on nonlinear analyses [9][10][11][12][13]. A comparison made between those connectors which have various Force/Deformation curves shows how much elastic/inelastic response of the frame strengthened by CLT is associated to the connector curve [2][8]. Stiffer connectors provide more stiffness and strength for the main frame, while energy dissipated by the connectors depends on the yielding displacement. Materials with low-yield displacement produce plastic loops with low load-carrying capacity under cyclic/seismic loadings. Also, the ones with high-yield displacement almost lack plastic loops. In both case, energy dissipated that is represented by the area inside the plastic loops is the lowest. It can be proved that there is a specific yielding point between these two extremities where the energy is

the greatest. Moreover, the locations of connectors along the frame are effective in changing the Dissipated Energy (DE), strength or drift of the frame [14]. The problem would have an economical advantage where, among different connectors with the same cyclic performance, the cheapest one can be adopted arranged optimally along the frame.

To find the values resulting in the most favourable response of the frame, an optimization process is carried out using Genetic Algorithm (GA) in binary form, which is a stochastic optimization technique based on the process of natural selection that belongs to the evolutionary algorithm [15]. It is considered as a powerful tool for discrete problems like here where optimum arrangement is sought, and the problems with high degree of nonlinearity where plastic deformations of different materials under dynamic loadings are evaluated.

In this study, a RC-CLT connector is represented by two perpendicular split and uplift springs where Force-Deformation curves are assumed to be bilinear for simplicity. The arrangement and yielding displacement of the connectors are obtained so that the strengthened frame has the highest dissipated energy and strength, and least drift in cyclic and seismic analysis, respectively, for both bare and masonry-infilled RC frames. In the final section, an economical survey is performed between two connectors with different stiffness and prices.

2 Modelling of the infilled RC frame coupled with CLT panel

The first step to proceed with the study's plan is to define and characterize the structure's elements and the renovation solution, and describe how to simulate them. Then, the optimization problem, including the

¹ Zabih Mehdipour, University of Minho, Portugal, zabih.mehdipour@gmail.com.

² Jorge M. Branco, University of Minho, Portugal, jbranco@civil.uminho.pt.

³ Elisa Poletti, University of Minho, Portugal, elisapoletti@gmail.com.

⁴ Paulo B. Lourenço, University of Minho, Portugal, pbl@civil.uminho.pt.

optimization algorithm, goal function, variables, constraints, will be defined clearly. The last step is to connect the frame strengthened with the optimization process. All aforementioned will be discussed as follows.

2.1 THE INFILLED RC FRAME COUPLED WITH CLT SHEAR WALL

Due to the nature of the problem, where the hybrid frame is analysed many times to achieve the optimal solution and nonlinear behaviour of materials (RC frame, masonry infill, and RC-CLT connector), the finite element analyses of the frame are carried out in OpenSees [16]. Figure 1 shows the geometry and reinforcement of the RC frame where the beams and columns cross-sections are, respectively, $160 \times 270 \text{ mm}^2$ and $160 \times 160 \text{ mm}^2$ with the rebars made of A400NR and concrete of class C55/67 [17].

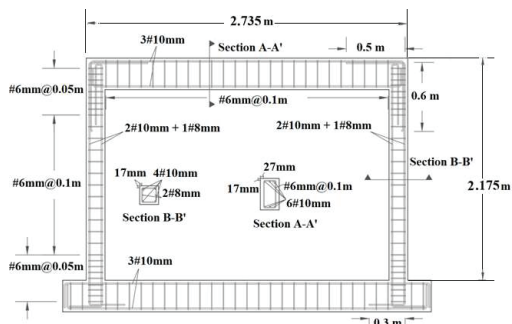


Figure 1: Reinforcement and geometry of the RC frame

In simulations, the beams were considered elastic, while the columns were constructed by FiberSection object, available in the software, governed by Concrete02 material assigned to concrete and Steel02 assigned to rebars as shown schematically in Figure 2.

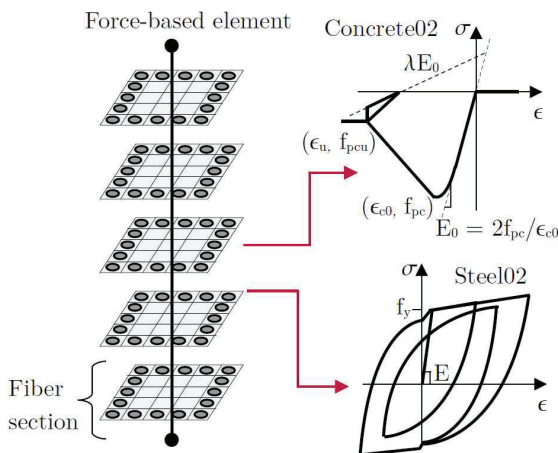


Figure 2: The materials assigned to the RC elements

In Table 1 and 2, calibrated parameters of Concrete02 and Steel02 material are presented, respectively. Figure 3 displays the cyclic response of the frame taken from the experimental [17] and numerical analysis, confirming the accuracy of materials used in modelling.

Table 1: The parameters for Concrete02 material

f_{pc} (MPa)	ϵ_{c0} (-)	f_{pcu} (MPa)	ϵ_u (-)	λ (-)	f_t (MPa)	E_{ts} (MPa)
31.20	0.002	6.24	0.05	0.005	4.36	436.5

Table 2: The parameters for Steel02 material

f_y (MPa)	E_0 (MPa)	b (-)	R_0 (-)	$cR1$ (-)	$cR2$ (-)
400	205000	0.015	10	0.94	0.20

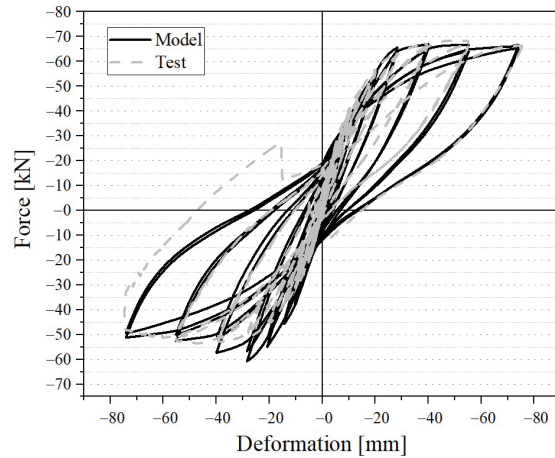


Figure 3: The frame cyclic behaviour in model and test

Also, masonry infill is made of vertically perforated masonry units reinforced in bed joints and connected to the RC columns in the interface by metallic connectors [17]. The panels are replaced with the solid parts, made of triangle solid beam elements, that are connected together by Zero-Length element assigned by Pinching4 element, as seen in Figure 4, [18] suitable to consider strength degradation and pinching effect typical of masonry walls due to crack openings. The equivalent scheme for the wall is shown in Figure 5 with the element governing horizontal spring in which the parameters reproduced by Genetic algorithm are listed in Table 3.

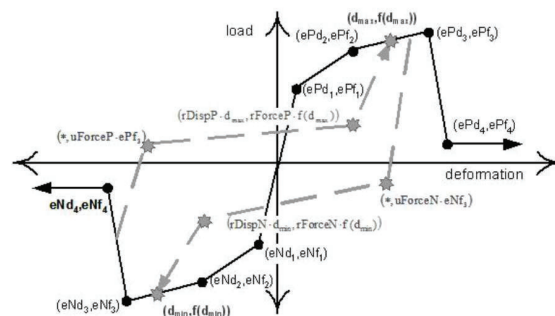


Figure 4: The behaviour of Pinching4 material

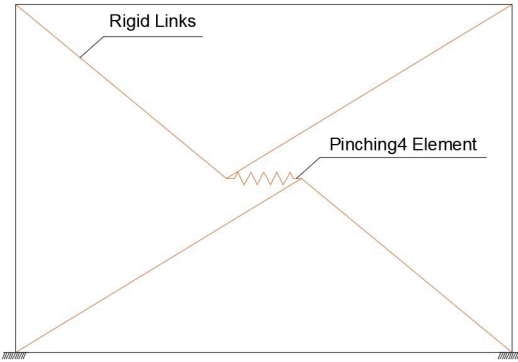


Figure 5: The masonry infill in modelling

Table 3: The parameters for Pinching4 material

Parameter	Value	Parameter	Value
ePf1 (MPa)	0.0736	fForceN (-)	0.2
ePf2 (MPa)	0.157	uForceN (-)	0.01
ePf3 (MPa)	0.196	gK1 (-)	1.3
ePf4 (MPa)	0.177	gK2 (-)	1.3
ePd1 (-)	0.0024	gK3 (-)	1.3
ePd2 (-)	0.014	gK4 (-)	1.3
ePd3 (-)	0.028	gKLim (-)	1.3
ePd4 (-)	0.0499	gD1 (-)	1
eNf1 (MPa)	-0.0736	gD2 (-)	1
eNf2 (MPa)	-0.1373	gD3 (-)	4
eNf3 (MPa)	-0.167	gD4 (-)	4
eNf4 (MPa)	-0.157	gDLim (-)	1
eNd1 (-)	0.0024	gF1 (-)	1
eNd2 (-)	0.014	gF2 (-)	0
eNd3 (-)	0.028	gF3 (-)	1
eNd4 (-)	0.0499	gF4 (-)	1
rDispP (-)	0.5	gFLim (-)	1
fForceP (-)	0.2	gE (-)	10
uForceP (-)	0.01	dmgType (-)	"energy"
rDispN (-)	0.5		

With the above-shown elements representing masonry infill, variation of base shear against peak displacement in the infilled frame resulted from test and simulation are similar (Figure 6).

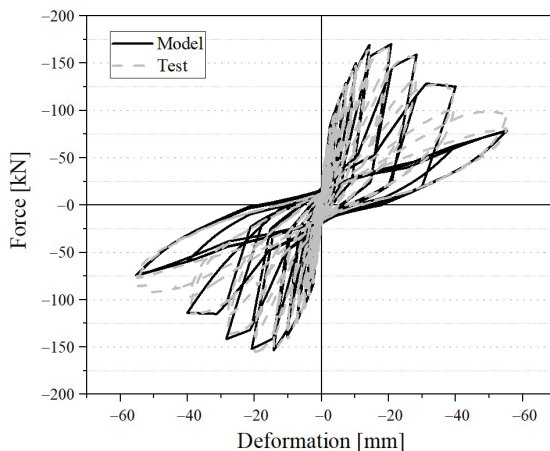


Figure 6: The infilled frame response in cyclic analyses

The CLT panel, used here, has 97 mm thickness in three layers, which are 35, 27, and 35 mm, respectively.

Because of the panel staying elastic in elastic analyses, only elastic moduli of elasticity, shear modulus, and Poisson's ratio need to be defined (Table 4), and are taken into account in simulations [19][20][21].

Table 4: The panel characteristics

Property	Value
E_L	11,000 N/mm ²
E_R	370 N/mm ²
E_T	370 N/mm ²
G_{LR}	688 N/mm ²
G_{LT}	688 N/mm ²
G_{RT}	68.8 N/mm ²
ν_{LR}	0.02
ν_{LT}	0.02
ν_{RT}	0.3

CLT shear wall generally are simulated in the same way as masonry infill did, meaning that, as shown in Figure 7, the wall is replaced by two frames made of solid beam elements at the top and bottom of the frame that attach CLT-frame connectors and a horizontal elastic shear spring at the middle of the wall, representing the CLT lateral stiffness.

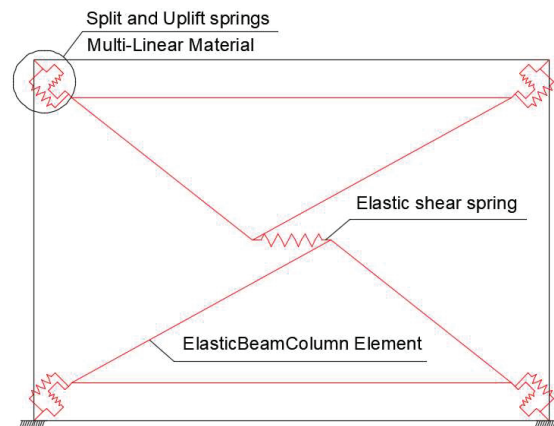


Figure 7: The panel with the connectors in the model

The stiffness of the mid-spring in Figure 7 is determined by the following equation [13]:

$$k_{CLT} = \frac{1}{\frac{h^3}{12EI} + \frac{1.2h}{GA}} \quad (1)$$

where h is the panel height, A is the cross-section area, I is the cross-section inertia, and E and G are the moduli of elasticity and shear modulus of the panel, respectively.

Both uplift and split springs that represent the connectors are usually attributed by Pinching4 or SAWS elements [22], but here to satisfy this study's purposes investigating bilinear spring, Multi-Linear material, available in the software library, is assigned to each of them comprising only two lines for simplicity. Stiffness of the second line is assumed as 10% of the first one. It can not be considered

as a separate optimization variable since it has a straight effect on increasing energy dissipated and strength.

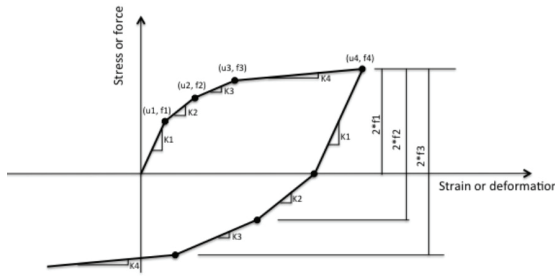


Figure 8: Multi-Linear material assigned to both split and uplift springs

2.2 THE OPTIMIZATION PROBLEM

It is supposed that only one kind of CLT-RC connection represented with split and uplift springs being characterized by bilinear Force-Deformation curves is used in the frame. Yielding displacement and elastic stiffness of the split and uplift springs are of four variables of the connector with the inelastic stiffness considered as 10% of the elastic one. Each of RC elements has 6, 8, and 10 potential locations where the connector can connect RC frame to the CLT panel. 6, 8, 10 spots per element (or 24, 32, 40, respectively, spots in total along the frame) are for the problem with 4, 8 and 12, and 16 and 20 connectors, respectively.

Number of possible locations of connectors along the frame, which are 24, 32, and 40, depending on the number of connectors, are of the variables assigned for the possible location of connectors, each of which can be 1, meaning there is the connector, or zero. Optimum locations and connector's properties are sought for specific number of connectors, that is, 4, 8, 12, 16 and 20. Number of population was assumed to be number of variables multiplied by 40. The lower and upper bound for elastic stiffness of springs are respectively 0.1 and 100 kN/mm and those of yielding displacement are 0.5 mm and 50 mm, respectively. For the problem where only spring's location is sought, elastic and inelastic stiffness of split springs are taken 3 and 0.5 and those of uplift springs are 2 and 0.6 kN/mm , respectively. Also, in the problem where only spring properties are demanded, optimum locations resulted from former analysis are considered for specific number of connectors. In the GA algorithm, for crossover, roulette wheel selection is used, and mutation coefficient is taken 0.2. The algorithm stops when the best answer stays unvaried for 15 iterations. For the sake of simplicity in expressing the variables, especially location of springs, binary genetic algorithm is adopted here meaning that all the variables in the population are expressed as binary numbers in the base-2 numeral system. Two loadings are applied to the bare/infilled frames: cyclic and seismic. The goal function is defined depending on the loading. Table 5 presents in summary all analyse with loading, goal function (GF), frame, and variables.

Table 5: Optimization problems studied here

No	Frame	Loadin	GF	Variables
.			g	

1	Bare	Cyclic	DE	Location/Propertie s
2	Bare	Cyclic	Strengt h	Location
3	Infille d	Cyclic	DE	Location/Propertie s
4	Infille d	Cyclic	Strengt h	Location
5	Bare	Seismic	DE	Location/Propertie s
6	Bare	Seismic	Drift	Location
7	Infille d	Seismic	DE	Location/Propertie s
8	Infille d	Seismic	Drift	Location

2.3 THE LOADINGS PROTOCOL

Two kinds of loadings, cyclic and seismic, are applied to the frame to figure out the dependency of them to the optimum arrangement and properties of the connectors. The loading pattern is obtained according to FEMA 461 [23] and has 16 steps, starting from 0.5 mm, regarding 0.026% drift, and ending in 75, regarding 3.94% drift. Each step is repeated two times with the exception of the first one repeating six times. Also, a set of six earthquake records as the seismic loading, mentioned in Table 6, is exerted on the structure.

Table 6: The seismic records [24]

Event Name	Station Name	Year
L'Aquila Italy	V. Aterno - Centro Valle	2009
Kocaeli Turkey	Izmit	1999
Manjil Iran	Abbar	1990
Kalamata Greece-01	Kalamata (bsmt)	1986
Corinth Greece	Corinth	1981
Friuli Italy-01	Barcis	1976

3 RESULTS AND DISCUSSIONS

3.1 OPTIMUM ARRANGMENT

The specific number of connectors (4, 8, 12, 16, and 20) was selected to be a multiple of 4 for regularity as there are four RC joints or four RC elements. In the first section optimum location to attach the panel along the RC frame is shown for those numbers of connectors with the specific properties, as mentioned before.

In the figures schematically shown as follows, the infilled squares show where the connector attach CLT and RC frame resulting in a better response, but cross signs are the potential locations of connectors which are not preferred. In case of using 4 connectors, in all cases, the best arrangement is displayed in Figure 9. As it is usually considered, four connectors in the corners, RC joints, give the most favorable response.

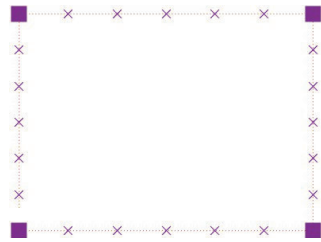


Figure 9: Optimal locations of 4 connectors

For 8 connectors, Figure 10 and 11 show the frame with the highest DE, and strength, respectively, under cyclic loading. In the seismic action, the optimal distribution is different from cyclic loading, but in both cases, connectors are located along the beams and columns in terms of DE and strength criteria.

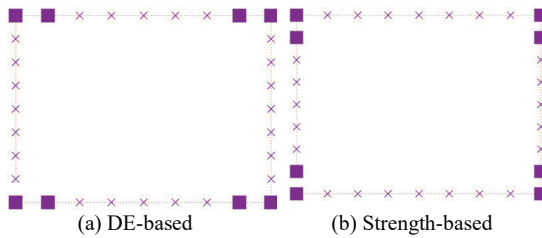


Figure 10: Optimal locations of 8 connectors under cyclic loading

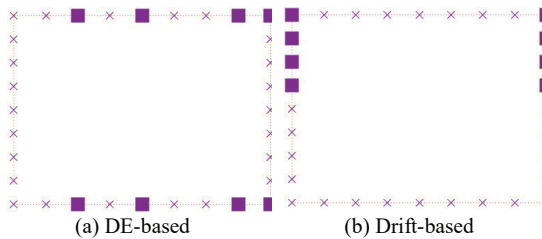


Figure 11: Optimal locations of 8 connectors under seismic loading

With the same order, Figures 12 and 13 demonstrate the connectors optimally arranged under cyclic and seismic loadings, respectively.

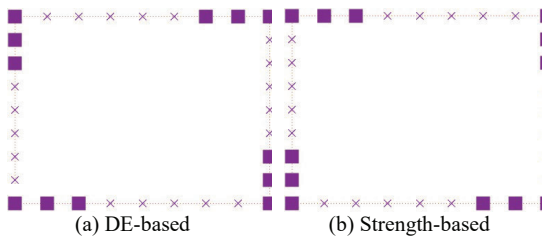


Figure 12: Optimal locations of 12 connectors under cyclic loading

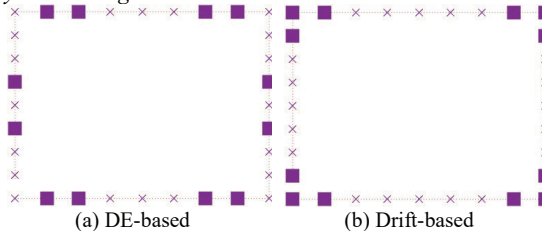


Figure 13: Optimal locations of 12 connectors under seismic loading

The following figures show the distribution of 16 connectors:

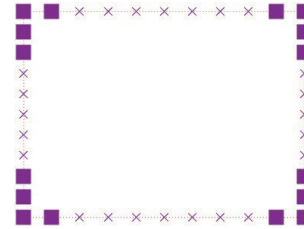


Figure 14: Optimal locations of 16 connectors under cyclic loading

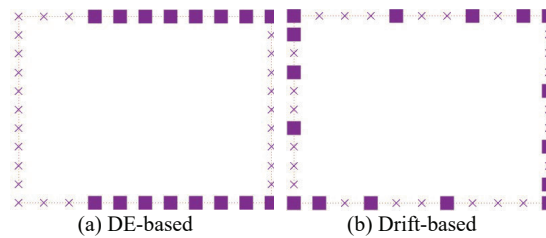


Figure 15: Optimal locations of 16 connectors under seismic loading

And finally, in the presence of 20 connectors, optimal positions of connectors are shown in the following figures:

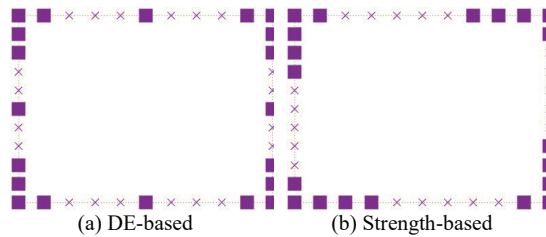


Figure 16: Optimal locations of 20 connectors under cyclic loading

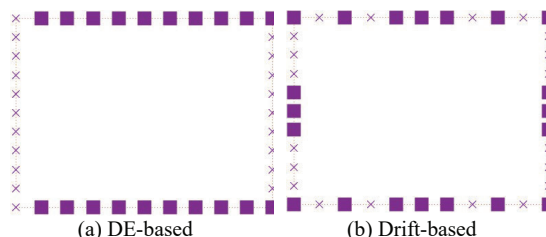


Figure 17: Optimal locations of 20 connectors under seismic loading

The first outcome shown in Figures 9 to 17 is that the optimum arrangement depends on the loading and the criteria used to determine it. That is, the DE of the structure under cyclic loading is completely different from the one under seismic action, or what is obtained as a result of having the highest DE is not the same as the highest strength or lowest drift. By classifying the

problem based on loadings and objective function, some general outlines are extracted: optimal connectors' positions in the frame under seismic loading are equal along the upper and lower beam, leading to the highest DE, while under cyclic loading, the connectors in the corners offer the best response. The connectors, however, often occupy the frame corners while there are few of them in order to achieve the lowest drift, but as their number increases, this ideal location shifts to along the beams. Finally, although usually more strength is associated with less drift, the optimal solution of the frame with the highest strength is not exactly the same as that for the frame with the lowest drift since the locations of the former are concentrated in the frame corners, regardless of their number.

3.2 OPTIMUM BI-LINEAR CURVE

As mentioned before, yielding displacement of connectors is the only feature of the springs on which the dissipated energy of the frame depends. There is a specific point of split and uplift yielding where the dissipated energy is the highest, as demonstrated in Figure 18 for the bare frame attached to the panel by four-in-corners connectors under cyclic loading. Searching all possible variables is time-consuming and adopting an optimization methodology is unavoidable. As mentioned section 3.1, this solution is sought here by GA. Table 7 and 8 present the optimal values of yielding displacements in the bare and infilled frames, respectively, for both horizontal and vertical springs in the presence of different specific even number of connectors, ranging from 4 to 20 optimally arranged along the frame as a result of previous subsection. Here only cyclic analysis was conducted since the seismic loading cannot necessarily push the frame until the yielding point, especially when the frame is equipped with higher number of connectors.

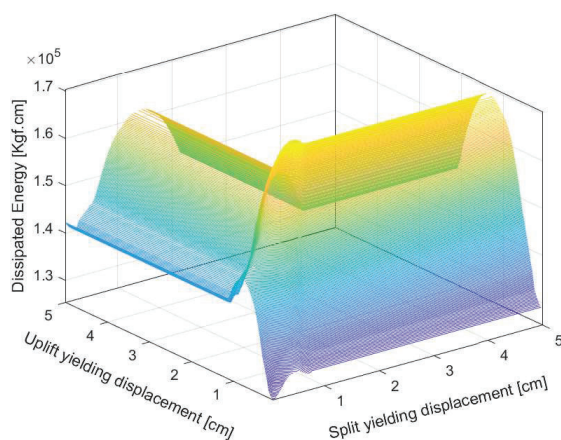


Figure 18: Energy dissipated versus yielding points of split and uplift springs

Table 7: Optimal yielding points of bare RC-CLT connectors

Connectors number	Split yielding point (cm)	Uplift yielding point (cm)
4	1.32	1.38
6	1.31	1.36
8	1.04	1.19

10	0.92	1.02
12	0.95	0.86
14	1.02	0.92
16	0.86	1.00
18	0.87	1.00
20	0.99	1.17

Table 8: Optimal yielding points of infilled RC-CLT connectors

Connectors number	Split yielding point (cm)	Uplift yielding point (cm)
4	1.31	1.47
6	0.95	1.73
8	1.24	1.40
10	1.29	1.58
12	1.42	1.53
14	1.21	1.80
16	1.58	1.49
18	1.13	1.94
20	1.39	1.65

Table 7 and 8 confirm that uplift yielding points are greater than split ones for both bare and infilled frames coupled to the panel by various numbers of connectors. Also, the corresponding split and uplift yielding displacements of the infilled frame strengthened is more than the bare frame for nearly all number of connectors. The average of split and uplift displacements of the reinforced bare frame are 1.03 and 1.10 cm, and those of the reinforced infilled frame are 1.28 and 1.62 cm, respectively.

3.3 ECONOMICAL CONNECTOR

After analysing the optimal yielding displacement and distribution of a specific connector with predefined elastic and inelastic stiffness, the next issue is to find out the connector with optimal stiffness. To achieve it, there needs to be a relationship between the stiffness and price of connectors. The research aims at analysing if a lesser number of stronger connectors (or more expensive ones) is more economical than a greater number of weaker connectors (or cheaper ones), considering an equal structural response with an optimal distributed. Due to lack of the stiffness-price relationship of connectors or a table including different connectors in terms of price and stiffness, the investigation here is summarized as follows comparing two connectors: a traditional angle bracket (AE116) and an innovative connection proposed by Rothblaas, so-called X-RAD. Tables 9 and 10 compare the price of each connector and their stiffness.

Table 9: The prices of two connections

Connector	Unit type	No.	Unit cost (€)	Total (€)
AE116	WBR90110	1	8.5	8.5
	LBA450	21	0.087	1.83
	Total cost (€)			10.33
XRAD	XONE	1	194	194
	XVGS1135	4	8.56	34.24
	0			
	MI120	1	105	105
	XBOLT166	8	2.91	23.28
5				

Total cost (€)	356.52
----------------	--------

Table 10: The stiffness of two connections

Connector	Stiffness	Split	Uplift
AE116	Elastic	2857.31	6448.89
	Inelastic	980.85	1008.86
X-RAD	Elastic	8675.80	20751.64
	Inelastic	1392.20	4374.79

A comparison is made between two cases; (1) four strong connectors (X-RAD) in the corners of the frame are installed; and (2) the number and distribution of the weaker one (AE116) is optimally found so that both cases result in an equal energy dissipation. The result shows that 16 AE116 connectors optimally distributed around the frame have approximately the same response, in terms of strength and dissipated energy (Figure 19), to the frame as 4 X-RAD connectors do. However, according to Table 9, the total material price of AE116 used is 165.28 (€), while X-RADs cost 1426.08 (€), confirming the importance of using connectors optimally designed both in number and mechanical properties in reducing expenses. Nonetheless, the former takes more time to be installed and this translates into increasing labour costs, thus resulting in a higher the total cost compared to X-RADs.

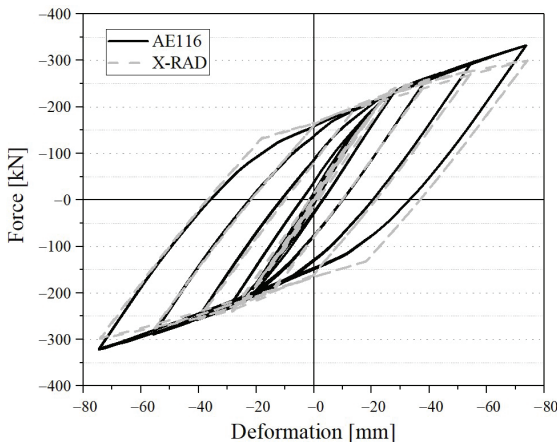


Figure 19: Force-Deformation of the reinforced frame for two cases

4 CONCLUSIONS

In this work, the optimum bilinear CLT-RC connectors on the one hand, and optimum configuration with certain numbers of those connectors on the other hand, were found. The outcome would be beneficial to design a real-case CLT-RC connector with the same properties as the one that was optimally attained here. This connector turned out to have a split and uplift yielding displacement of 1.03 and 1.10 cm for the CLT-infilled RC frame, and 1.28 and 1.62 cm for the masonry-infilled frame coupled with externally added CLT panel, respectively. It was observed that their placements are affected by both loadings and objective functions, though generally, no matter how many of them are utilized, the highest DE and strength are produced by corner-distributed connectors under cyclic loading, whereas the highest DE is produced by along-beam-distributed connectors under seismic

loading. In the case of the lowest drift in the frame, both distributions were observed.

ACKNOWLEDGEMENT

This work was financially supported by the Portuguese Science Foundation (Fundação de Ciência e Tecnologia, FCT) under the research project TimQuake - Structural performance of timber joints and structures under earthquakes (015/TT/2021).

REFERENCES

- [1] I. Sustersic and B. Dujic, "Seismic shaking table testing of a reinforced concrete frame with masonry infill strengthened with cross laminated timber panels," 2014.
- [2] Z. Mehdipour, J. M. Branco, I. Sustersic, L. G. Rodrigues, and P. B. Lourenço, "Masonry-infilled RC frames strengthened with cross-laminated timber panels," in *COMPdyn Proceedings*, 2021, vol. 2021-June.
- [3] A. B. Mehrabi and P. B. Shing, "Finite Element Modeling of Masonry-Infilled RC Frames," *J. Struct. Eng.*, vol. 123, no. 5, 1997, doi: 10.1061/(asce)0733-9445(1997)123:5(604).
- [4] I. Koutromanos, A. Stavridis, P. B. Shing, and K. Willam, "Numerical modeling of masonry-infilled RC frames subjected to seismic loads," in *Computers and Structures*, 2011, vol. 89, no. 11–12, doi: 10.1016/j.compstruc.2011.01.006.
- [5] I. Gavric, M. Fragiaco, and A. Ceccotti, "Cyclic Behavior of CLT Wall Systems: Experimental Tests and Analytical Prediction Models," *J. Struct. Eng.*, vol. 141, no. 11, 2015, doi: 10.1061/(asce)st.1943-541x.0001246.
- [6] V. Hristovski, V. Mircevska, B. Dujic, and M. Garevski, "Comparative dynamic investigation of cross-laminated wooden panel systems: Shaking-table tests and analysis," *Adv. Struct. Eng.*, vol. 21, no. 10, 2018, doi: 10.1177/1369433217749766.
- [7] M. Izzi, D. Casagrande, S. Bezzi, D. Pasca, M. Follesa, and R. Tomasi, "Seismic behaviour of Cross-Laminated Timber structures: A state-of-the-art review," *Engineering Structures*, vol. 170, 2018, doi: 10.1016/j.engstruct.2018.05.060.
- [8] Z. Mehdipour, E. Poletti, J. M. Branco, and P. B. Lourenço, "Numerical Analysis of Masonry-Infilled RC-CLT Panel Connections," *Buildings*, vol. 12, no. 11, 2022, [Online]. Available: <https://doi.org/10.3390/buildings12112009>.
- [9] J. Schneider, E. Karacabeyli, M. Popovski, S. F. Stierner, and S. Tesfamariam, "Damage Assessment of Connections Used in Cross-Laminated Timber Subject to Cyclic Loads," *J. Perform. Constr. Facil.*, vol. 28, no. 6, 2014, doi: 10.1061/(asce)cf.1943-5509.0000528.
- [10] F. T. Matos, J. M. Branco, P. Rocha, T. Demschner, and P. B. Lourenço, "Quasi-static tests on a two-story CLT building," *Eng. Struct.*, vol. 201, 2019, doi: 10.1016/j.engstruct.2019.109806.
- [11] G. D'Arenzo, W. Seim, and M. Fossetti,

- “Experimental characterization of a biaxial behaviour connector for CLT wall-to-floor connections under different load directions,” *Constr. Build. Mater.*, vol. 295, 2021, doi: 10.1016/j.conbuildmat.2021.123666.
- [12] A. Polastri and A. Angeli, “An innovative connection system for CLT structures: Experimental-numerical analysis,” 2014.
- [13] A. Aloisio, M. Pellicciari, S. Sirotti, F. Boggian, and R. Tomasi, “Optimization of the structural coupling between RC frames, CLT shear walls and asymmetric friction connections,” *Bull. Earthq. Eng.*, vol. 20, no. 8, 2022, doi: 10.1007/s10518-022-01337-8.
- [14] C. Aranha, J. Branco, P. Lourenço, G. Flatscher, and G. Schickhofer, “Finite element modelling of the cyclic behaviour of CLT connectors and walls,” 2016.
- [15] R. L. Haupt and S. E. Haupt, *Practical genetic algorithms*. 2004.
- [16] S. Mazzoni, F. McKenna, M. Scott, and G. Fenves, “OpenSees Command Language Manual,” *Pacific Earthq. Eng. Res. Cent.*, vol. 264, no. 1, 2006.
- [17] L. M. Silva, G. Vasconcelos, P. B. Lourenço, and F. Akhoundi, “Seismic performance of Portuguese masonry infill walls: From traditional systems to new solutions,” in *COMPADYN Proceedings*, 2019, vol. 2, doi: 10.7712/120119.7063.19702.
- [18] L. N. Lowes, N. Mitra, and A. Altoontash, “A Beam-Column Joint Model for Simulating the Earthquake Response of Reinforced Concrete Frames,” *Peer2003/10*, vol. 88, no. 4, 2003.
- [19] DIN 1052:2008 Entwurf, *Berechnung und Bemessung von Holzbauwerken – Allgemeine Bemessungsregeln und Bemessungsregeln für den Hochbau*. .
- [20] EN 338:2003, *Structural timber - Strength classes*. 2003.
- [21] J. Bodig and B. Jayne, *Mechanics of Wood and Wood Composites*. New York, USA: Van Nostrand Reinhold, 1982.
- [22] Y. L. Shen, J. Schneider, S. Tesfamariam, S. F. Stiemer, and Z. G. Mu, “Hysteresis behavior of bracket connection in cross-laminated-timber shear walls,” *Constr. Build. Mater.*, vol. 48, 2013, doi: 10.1016/j.conbuildmat.2013.07.050.
- [23] F. E. M. A. (FEMA), “Interim Protocols For Determining Seismic Performance Characteristics of Structural and Nonstructural Components Through Laboratory Testing,” *FEMA 461*, no. June. 2007.
- [24] T. Ancheta, R. Darragh, J. Stewart, and E. Seyhan et al., “PEER 2013/03: PEER NGA-West2 Database,” Pacific earthquake engineering research center (PEER), 2013. doi: <http://peer.berkeley.edu/publications/>.